Cluster-cluster aggregation with mobile impurities

Anwar Hasmy, Juan Primera, Thierry Woignier

Cluster–cluster aggregation with mobile impurities

Anwar Hasmy[1] · Juan Primera[2,3] · Thierry Woignier[4,5]

Abstract

We considered the diffusion-limited cluster–cluster aggregation (DLCA) model in the presence of inert template (mobile impurities) for the simulation of mesoporous materials obtained through sol–gel processes. A computer algorithm based on the off-lattice version of the two-dimensional DLCA model with moving impurities is introduced. If the density of monomers is large enough, a porous matrix results at the end of the aggregation mechanism. Impurities are removed at the final stage of the simulation, assuming that the porous structure is not altered as in some experiments. We are interested in the modification of the resulting porous structure due to the presence of moving inert impurities during aggregation. The resulting porous material consists of a homogeneous structure of interconnected fractal clusters. Such structure is characterized by computing the correlation length and the fractal dimension of these clusters. The numerical analysis of the pore size distribution reveals a strong dependence with the density and sizes of mobile impurities. Compared to the DLCA model, the curve distribution becomes bimodal when impurities are introduced, i.e., it appears a first maximum at small pore sizes (of the order of the monomer dimension), and a second maximum around the impurity size. For large monomer densities the amplitude of the peak around the impurity size becomes larger than the peak of the smallest pore size.

✉ Anwar Hasmy
anwarhasmy@hotmail.com

[1] Departamento de Física, Universidad Simón Bolívar, Valle de Sartenejas, Caracas, Venezuela

[2] Facultad de Ingeniería Agricola, Universidad Técnica de Manabí, Lodana, Manabí, Portoviejo, Ecuador

[3] Departamento de Física, FEC, Universidad del Zulia, Maracaibo, Venezuela

[4] Aix Marseille Univ, Univ Avignon, CNRS, IRD, IMBE, Marseille, France

[5] IRD UMR 237, Campus Agro Environnemental Caraïbes, B.P. 214 Petit Morne, 97232 Le Lamentin, Martinique

Graphical Abstract

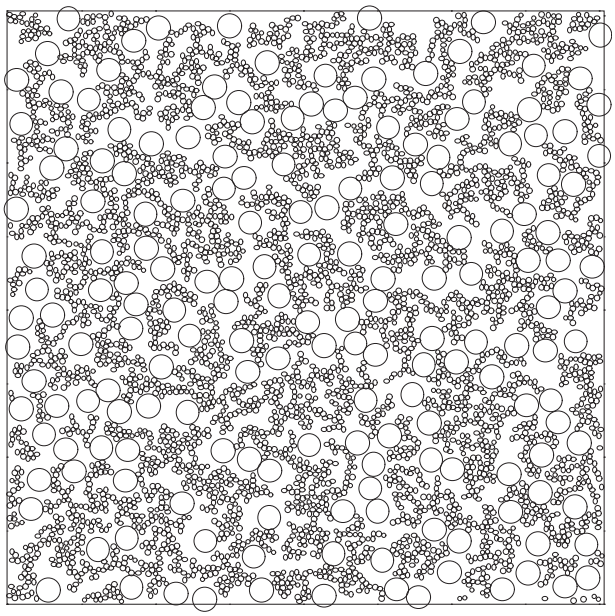

Highlights

- We simulate the mesoporous materials obtained through so–gel process by a cluster–cluster aggregation model in the presence of impurities.
- We show that the porous material consists of interconnected fractal clusters.
- The pore size distribution is strongly dependent on the concentration and the size of impurities.

Keywords Cluster–cluster aggregation · Numerical simulation · Template · Pore size distribution

1 Introduction

Colloidal aggregation phenomenon is present in a wide variety of systems that includes silica gels [1, 2], liposomes [3], metallic nanoparticles [4] and water in oil emulsions [5], among others. In some cases, the aggregation process is used for the fabrication of mesoporous materials for different applications, mainly due to the resulting very high specific surface area. Some of these applications include their use as catalyser support which have helped to improve the efficiency of the synthesis processes of a large variety of products, and also these materials are useful in the pharmaceutical, coating and chemical industry. The possibilities of control pore shapes and pore distributions include the use of template to tailor the system and open porous structure. In fact, it has been demonstrated that the use of template can affect the pore structure and their orientation [6–9].

One of the commonly used procedure for the fabrication of these materials is the sol–gel technique. In the last decades, surfactants started to be included in the solution for the corresponding material preparation, because they allow some control on the pore structure of the resulting objects [6, 7]. The surfactants form micelles which act as inert template during the monomer aggregation process until a macroscopic cluster is formed. Then, typically the micelles are roasted and the solvent extracted by evaporation or other drying technique. Depending on the chemical properties of the surfactant, the method can produce a solid material with a regular arrangement of cylinders (i.e., mesoporous Mobil Composition of Matter (MCM)), or a disorder porous network. For the disordered case, studies of the porous structure dependence on template features lack in the literature, and most of the numerical studies on mesoporous materials as carbon aerogels have been modeled by neglecting the formation dynamics of the sample [10].

On the other hand, cluster–cluster aggregation model has been used to simulate a large variety of phenomena, and it has been of much interest in the study of colloidal aggregation [11, 12]. For instance, this type of models has been successful in describing the dynamics and the final structure of gels formed on base catalyzed and colloidal conditions [1, 13, 14] as well as for many aerosol properties [15]. Similarly, cluster–cluster aggregation models have been used for the simulation of binary and multicomponent mixtures [16–21]. In particular, the on-lattice version of the diffusion-limited cluster-cluster aggregation (DLCA) model

has been used to study the aggregation in presence of mobile impurities of similar monomer sizes [20]. Nevertheless, to our knowledge, not the effect of the size of impurities, neither the effect of these impurities on the pore sizes distribution of the sample have been analyzed with this kind of models.

In this work, our main objective is to investigate the structural properties of a binary mixture consisting of inert mobile component, to mimic the effect of the template during the aggregation process, and of monomer species that can aggregate to form a macroscopic porous network. The monomer species and mobile impurities essentially can have arbitrary diameters. The model of aggregation used in this study is the *off-lattice* version of the diffusion-limited cluster–cluster aggregation (DLCA) adjusted to deal with mixtures. To reach such a goal with reasonable computational efforts, we have restricted our study to the two-dimensional model. However, we are convinced that the conclusions coming out from this study would be also valid to three-dimensional counterpart of the model in question. We show that the presence of mobile impurities and his respective size has profound influence on the porous network structure formed by the aggregation of monomers. In section II we describe details of the computer model considered for the mesoporous material simulation. The results and discussion are presented in section III, and finally we summarize the principal findings of this work.

2 The model and methodology

The aggregation model implemented in this work is based on the off-lattice extension [1] of the original DLCA model [22, 23], in two dimensions, but additionally to the initial random dispersion of monomers in a square box, we add inert impurities. Both monomers and impurities are chosen to be circular. Overlaps between monomers and/or impurities are forbidden. Then, the binary mixture consists of aggregating and inert mobile components. Monomers belonging to the aggregating component are characterized by their radius R_m and the packing fraction $\phi_m = \pi N_m R_m^2/L^2$, where N_m is the number of monomers in the square simulation box with the edge L. On the other hand, impurities are circular particles with radius R_t (which here is variable), and are considered at packing fraction $\phi_t = \pi N_t R_t^2/L^2$, with N_t and R_t denoting the number and radius of impurities, respectively.

Both the monomers particles and impurities diffuse randomly in the two-dimensional space among the directions (±1, ±1) with a step of the diameter size of monomers. When aggregating monomers become in contact, they stick together to form a cluster, and so on. Every collision between monomers results in the formation of a higher-order cluster entity. A cluster are chosen randomly for a motion, according to the respective diffusion coefficient, which is inversely proportional to the radius of gyration. A similar criterion was considered for the mobility of impurities. Since impurities are inert they preserve their initial radii, while the aggregating component grows until a macroscopic gel is formed, i.e., a system is built with an approximately size of the box. The impurities constitute obstacles for collisions between monomers, limiting aggregation, a reason of why the aggregation is slower than the pure DLCA case. In some limit situations, impurities could confine some of the aggregating clusters, preventing them to join the forming macroscopic gel. The simulation is stopped when the number of clusters does not reduce more, after a reasonable number of iteration or motion trials are performed.

We point out that we do not establish a gel criterion as in ref. [20], which drove to the phase diagram reported by those authors. The reason is that we are mainly interested in the global structure of the resulting object. In fact, it has been shown that the material structure obtained at the gel time (the time where appears the first cluster that expands from one side to the other opposite side of the box) is almost similar than that obtained at the end of the aggregation process, i.e., where all clusters and monomers form a single connected network [24]. In other words, for large time enough, the bonding or not between clusters does not alter too much the gel structure.

In Fig. 1 we show a snapshot of the system structure which describes the final stage of the simulation process with the following parameters: $\phi_m = 0.173$, $\phi_t = 0.226$,

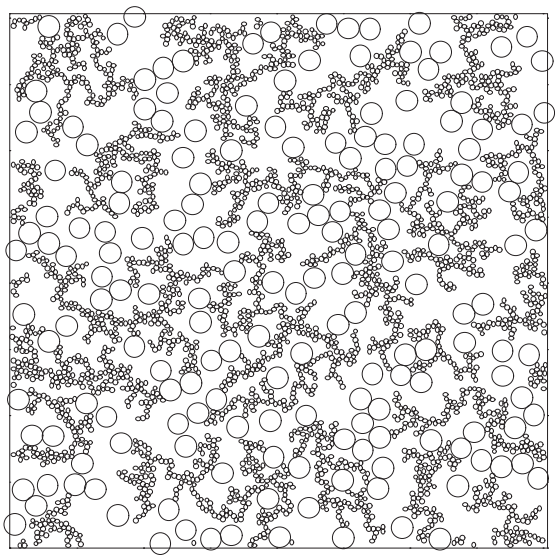

Fig. 1 Final configuration of aggregated via diffusion-limited cluster—cluster aggregation (DLCA) monomers (small circles) and inert impurities (big circles) in the simulation box at $\phi_m = 0.173$, $\phi_t = 0.226$, and $R_t = 4$

$R_t = 4$. Small and big circles correspond to monomers and impurities, respectively. One can observe that impurities are uniformly distributed in the box, the aggregating monomers formed several clusters (whereas the two snapshots in the bottom of Fig. 9 show that the aggregating subsystem is quite close to form a gel, i.e., a spanning cluster going from one side to the other side of the box is formed).

In this work, all the results come out from our calculations in the square box with $L_x = L_y = L = 200$. Periodic boundary conditions have been implemented along x- and y-axes. The radius of impurities is a parameter chosen equal to 1, 2, 4, or 8, whereas the monomer radius $R_m = 0.867$. As done in mesoporous material fabrication, the resulting structure is analyzed after the impurities are removed.

3 Results and discussion

For a quantitative analysis of the structure of the simulated porous materials, we calculated the correlation or pair distribution function of monomers $g(r)$ such that $g(r)\ d^2r$ is proportional to the probability of finding a particle center in an area d^2r at a distance r from a given particle center. Therefore, for an isotropic material, the number of particle centers dn located between r and $r + dr$ from a given particle center is proportional *to* $g(r)2\pi r dr$. Since in average the number of particle centers per unit volume is $\phi_m/\pi {R_m}^2$, one can normalize $g(r)$ to unity when r tends to infinity, by doing [1]:

$$dn = \frac{\phi_m}{\pi R_m^2} g(r) 2 r dr = \frac{2\phi_m}{R_m^2} g(r) r dr. \qquad (1)$$

The three $g(r)$ curves presented in Fig. 2 correspond to fixed monomer density $\phi_m = 0.173$ and variable density of impurities, $\phi_t = 0$, $\phi_t = 0.15$, and $\phi_t = 0.226$, and the impurity radius is fixed, $R_t = 4$. An obvious effect of increasing the density of impurities on the monomer distribution is the shift of the minimum of $g(r)$ to smaller distances. This minimum represents the characteristic maximum size ξ of fractal clusters of dimension D_f, since for $1 < r < \xi$, the number of monomers N_m scales as r^{Df} [1]. Such characteristic length ξ is hereafter called the correlation length. Smaller clusters are formed in the system with impurities, when it is compared to the system without impurities. In all cases, however, fractal objects are formed. The fractal dimension of clusters and the corresponding values of the correlation length are given in Fig. 3. The effect of increasing the density of impurities at given monomer concentration is to decrease the fractal dimension of clusters consisting of monomers as previously obtained in ref. [19] (see open symbols). However, we observe that this is accompanied with a monotonic decrease of the correlation length ξ of fractal clusters (black symbols). On the other hand, the subsystem of impurities provides certain

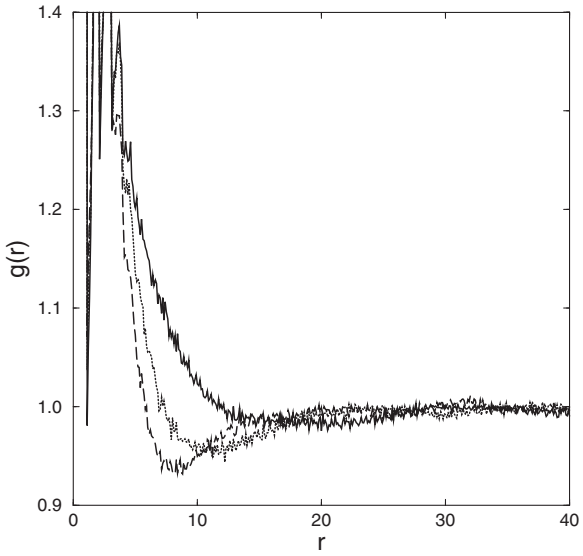

Fig. 2 Effect of impurity concentration on the monomer–monomer pair distribution function, $g(r)$, in the system consisting of monomers at fixed density $\phi_m = 0.173$, and at $\phi_t = 0$ (solid line), $\phi_t = 0.15$ (dotted line), and $\phi_t = 0.226$ (dashed line). In all cases radius of impurities is fixed at $R_t = 4$

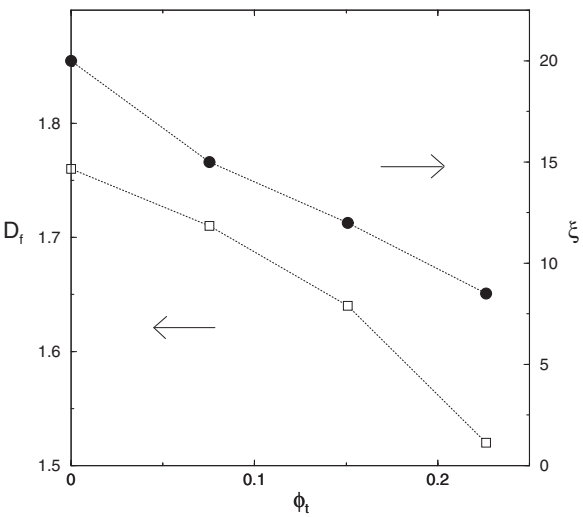

Fig. 3 Dependence of the fractal dimension of aggregates D_f (empty squares) and of correlation length ξ (filled circles) on density of impurities at $\phi_m = 0.173$, $R_t = 4$

excluded volume and consequently the area in which monomers diffuse is reduced, in comparison to the case without impurities. This effect can result in the increasing effective probability of collisions between monomers. The structure of clusters formed via aggregation in the presence of impurities will also be affected.

As mentioned above, we are interested in changes of the pore structure due to the presence of impurities. We define the pore size distribution (PSD) function $f(R)$ as the fraction of volume corresponding to the spherical pore of radius R.

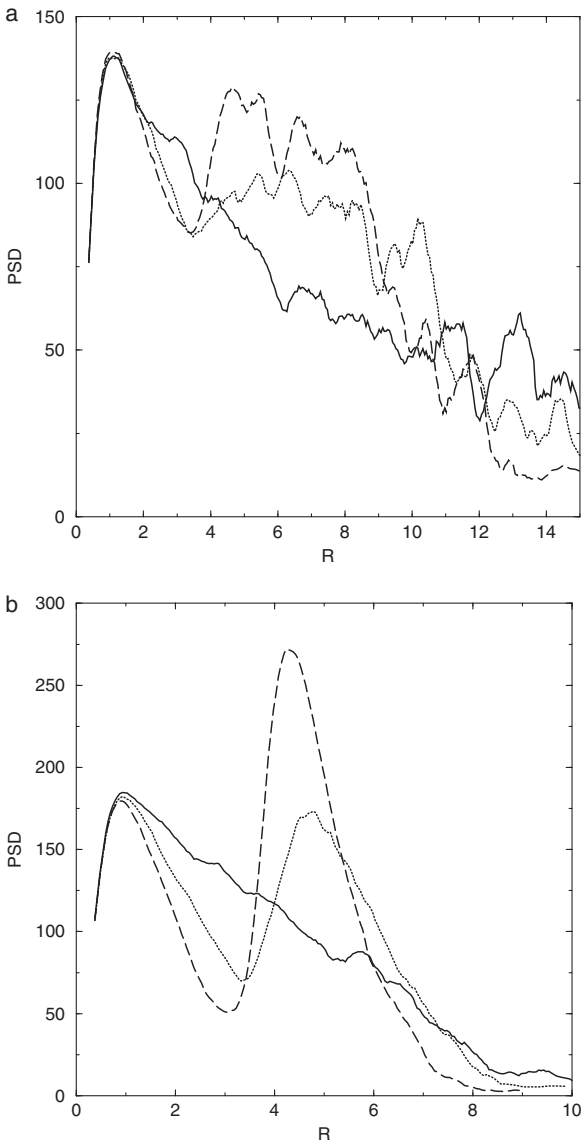

Fig. 4 The pore size distribution (PSD) versus pore radius R. **a** Effects of density of impurities on PSD at $\phi_m = 0.173$, $R_t = 4$; the solid, dotted, and dashed lines correspond to $\phi_t = 0$, $\phi_t = 0.15$, and $\phi_t = 0.226$, respectively. **b** The same as in **a**, but at $\phi_m = 0.26$. In both (**a**, **b**) the results are for $R_t = 4$

In order to obtain $f(R)$, first we calculate a cumulative volume, $v(R)$, as the total volume occupied by, as many as possible, test spheres of radius R, and smaller in the applied simulation box. The cumulative volume is constructed in the form of a histogram. All the test spheres do not overlap with aggregating monomers and moreover do not overlap between themselves. The PSD then is determined by:

$$f(R) = \frac{1}{L^2}\frac{dv(R)}{dR}. \qquad (2)$$

Since our simulations are in two dimensions, v(R) represents the cumulative area instead of volume. The resulting curves are reported in arbitrary units.

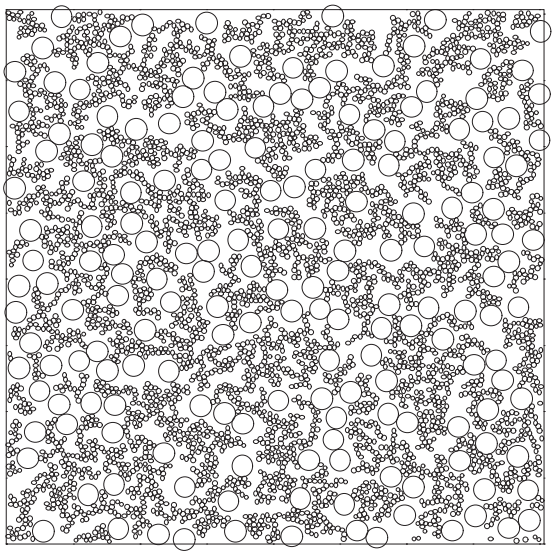

Fig. 5 Final configuration of aggregated monomers (small circles) and inert impurities (big circles) in the simulation box at $\phi_m = 0.26$, $\phi_t = 0.226$, $R_t = 4$. The pore size distribution (PSD) of this system is given by the dashed line in Fig.4b

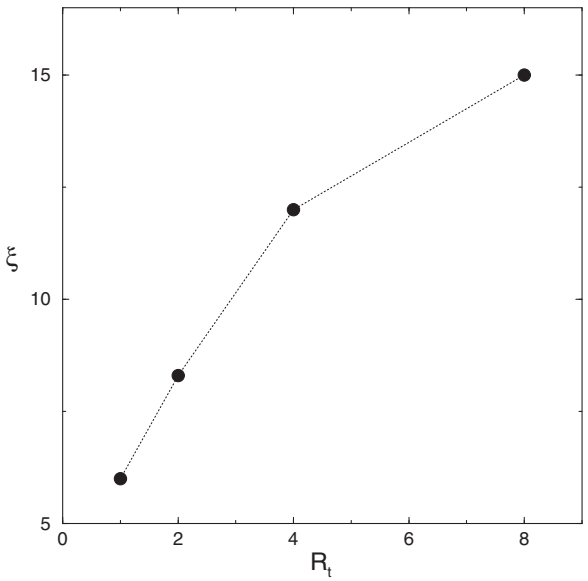

Fig. 6 Dependence of the correlation length ξ on impurity radius at fixed monomer density $\phi_m = 0.173$ and fixed density of impurities $\phi_t = 0.15$

The effect of the density of impurities on the PSD is shown in Fig. 4. The Fig. 4a compares the case without impurities, where the PSD has a single maximum corresponding to small pores of the radius $R = 1/2$. For bigger R values, the PSD function decreases as expected. For two systems with impurities we observe development of an additional maxima roughly corresponding to bigger pores $R > 4$, while the impurity radius is 4. This tendency becomes stronger with increasing the density of impurities.

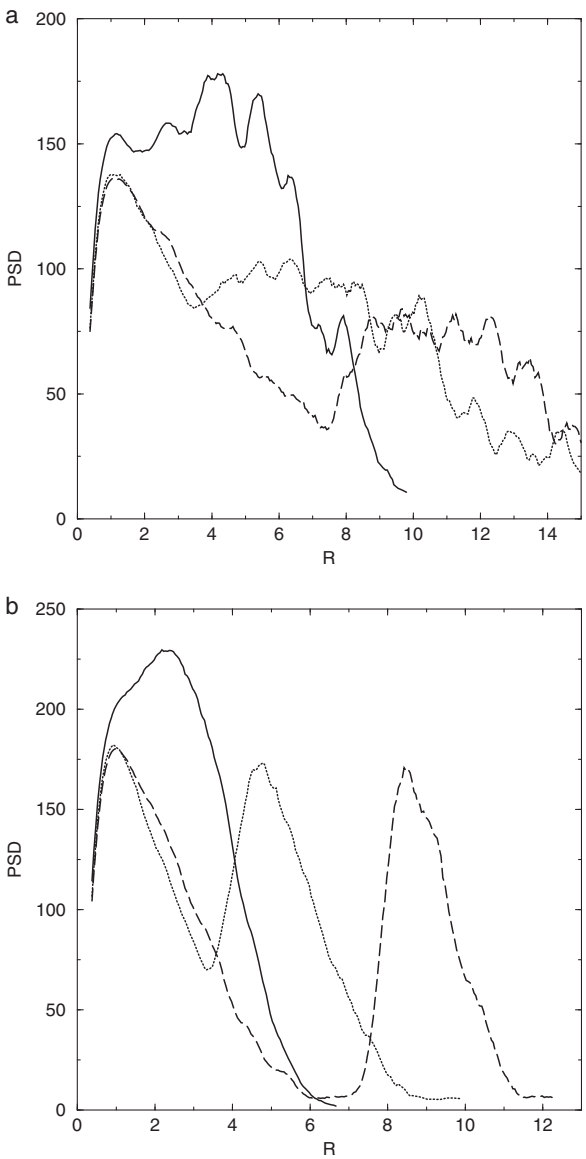

Fig. 7 The pore size distribution (PSD) versus pore radius R. **a** The effects of impurity radius on PSD at $\phi_m = 0.173$, $\phi_t = 0.15$; the solid, dotted, and dashed lines correspond to $R_t = 1$, $R_t = 4$, and $R_t = 8$, respectively. b The same as **a**, but at $\phi_m = 0.26$

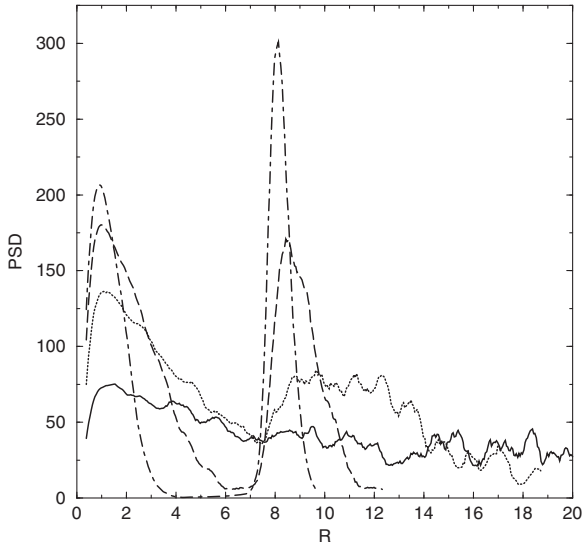

Fig. 8 The pore size distribution (PSD) versus pore radius R. Effects of monomer concentration on PSD at $\phi_t = 0.15$, $R_t = 8$. The solid, dotted, dashed, and dash-dotted lines correspond to $\phi_m = 0.087$, $\phi_m = 0.173$, $\phi_m = 0.26$, and $\phi_m = 0.347$, respectively

A well-pronounced maximum for $R = 1/2$ is nevertheless preserved. One must have in mind that chosen monomer density is not high, $\phi_m = 0.173$, and there remains enough space in the system which is not affected by the presence of impurities in the growth procedure. At higher monomer density, $\phi_m = 0.26$, trends for the development of pores corresponding to removed impurities for the system are very much stronger (Fig. 4b). Additionally, one can observe that the second peak of the PSD seems to slightly decrease to smaller pore size values (dotted to dashed) for increasing impurity volume fraction. Now, we have good evidence that the pores with the radius corresponding to impurities are present in the system. Moreover, if the density of impurities is higher, the fraction of such pores overwhelms the fraction of small pores, an effect that can be observed in Fig. 5.

Besides, we have performed several computational runs to investigate the effect of impurities radius on the final structure and its PSD. In this case we have considered intermediate monomer density, $\phi_m = 0.173$, similar to the system investigated in Figs. 1–3. However, we considered a fixed value for the density of impurities, $\phi_t = 0.15$, and only the impurity radius is varied. The dependence of the correlation length ξ on the impurities radii is shown in Fig. 6. Increasing the impurity radius at fixed monomer packing fraction evidence the formation of large clusters, which may or may not have fractal structure, because for such monomer packing fraction (and higher), the fractal dimension tends to the spatial dimension.

Figure 7 shows the PSD function for a density of impurities ϕ_t equal to 0.15, and impurity radii equal to 1 (solid curves), 4 (dotted curves), and 8 (dashed curves). The monomer density ϕ_m is equal to 0.173 (Fig. 7a) and 0.26 (Fig. 7b). The analysis of Fig. 7a evidences that impurities with $R = 1$ produce a porous material with prevailing small and intermediate size pores, whereas smaller number of big impurities yields porous material with decreasing number of small pores and certain fraction of much bigger pores. Such effects on the PSD function become stronger as the initial concentration of monomers increases as shown in Fig. 7b.

We also addressed the effect of monomer concentration on the porosity of the material with impurities at a fixed density of impurities, $\phi_t = 0.15$, and fixed impurity radius,

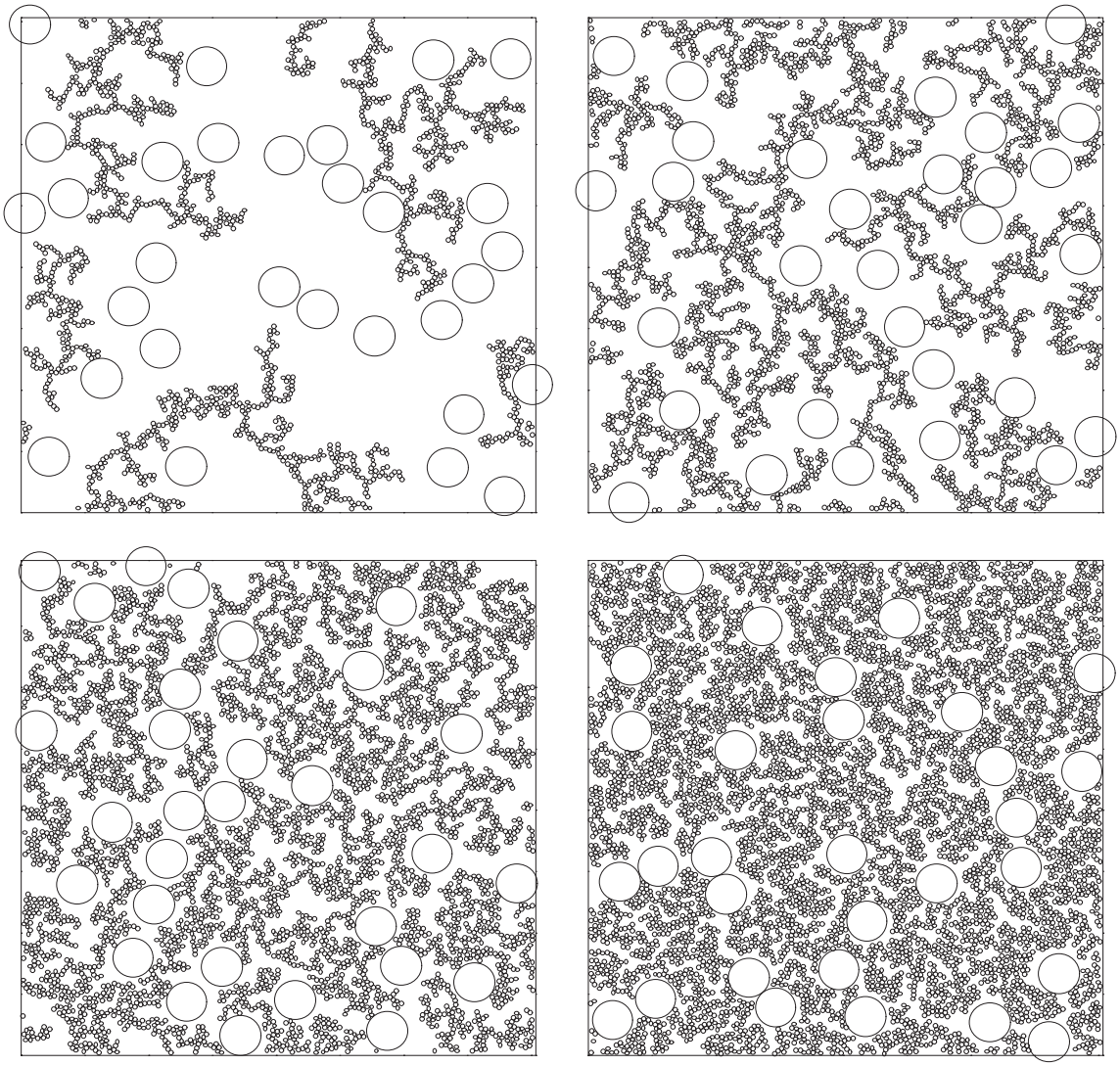

Fig. 9 Final configurations of aggregated monomers (small circles) and inert impurities (big circles) in the simulation box at $\phi_m = 0.087$ (top left), $\phi_m = 0.173$, $\phi_m = 0.26$, and $\phi_m = 0.347$, four panels according to the increasing number of small circles. The template parameters are fixed: $\phi_t = 0.15$, $R_t = 8$. The PSD of these four systems are those given in Fig. 8

$R_t = 8$. The PSD function at four values of the monomer concentration is shown in Fig. 8, whereas the snapshots of the particle configurations in the box corresponding to these functions are shown in the four panels of Fig. 9. When the monomer density is increased, the results in Fig. 8 show that the PSD develops two maxima. The first peak reflects the presence of small pores of the order of the monomer size (corresponding the same maximum of the case without impurities) but slightly larger. The second peak reflects the presence of big pores due to impurities, whose size results very close to the value of the impurity radius. Additionally, it is observed that such peak become sharper as the monomer densities increase and that the fraction of big pores overwhelms fraction of small pores.

4 Conclusion

We have shown that for a binary mixture consisting of inert mobile impurities and monomer species that can aggregate, the resulting final gel structure exhibits a correlation length that decreases as the concentration of impurities increases, as well as the size of impurities decreases. These changes in the correlation length with concentration and size of the impurities can be understood in terms of the space left free due to aggregation and gelation process of monomers and clusters. On the other hand, the increase in the concentration and size of impurities produces the appearance of a second peak in the PSD that tends towards higher values as concentration and size of impurities increase. Such finding

could be expected since the impurities induce a void in the space of the order of their sizes that modify the resulting porous structure. Finally, extension of the model to three dimensions is straightforward, but intuitively one can assume that qualitative results obtained here can be generalized to the three-dimensional situation.

References

1. Hasmy A, Anglaret E, Foret M, Pelous J, Jullien R (1994) Small-angle neutron-scattering investigation of long-range correlations in silica aerogels: Simulations and experiments. Phys Rev B 50:6006–6016
2. Woignier T, Phalippou J. (2016) Glasses: sol–gel methods. In: Hashmi S. (ed) Reference module in materials science and materials engineering. Elsevier Inc., Amsterdam p 3581–3585
3. Sabín J, Prieto G, Ruso JM, Messina P, Sarmiento F (2007) Aggregation of liposomes in presence of La 3+: a study of the fractal dimension. Phys Rev E 76:011408
4. Gao J, Qu R, Tang B, Wang C, Ma Q, Sun C (2011) Control of the aggregation behavior of silver nanoparticles in polyurethane matrix. J Nanopart Res 13:5289–5299
5. Fuller GT, Considine T, Golding M, Matia-Merino L, Mac Gibbon A, Gillies G (2015) Aggregation behaviour of crystalline oil-in-water emulsions: Part II – effect of solid fat content and interfacial film composition on quiescent and shear stability. Food Hydrocoll 43:521–558. 2015
6. Nishihara H, Iwamura S, Kyotani T (2008) Synthesis of silica-based porous monoliths with straight nanochannels using an ice-rod nanoarray as a template. J Mater Chem 18:3662–3670
7. Wa L, Fengyunb L, Fanlua Z, Mengjing C, Qianga C, Jueb H, Weijunc Z, Mingweia M (2015) Preparation of silica aerogels using CTAB/SDS as template and their efficient adsorption. Appl Surf Sci 353:1031–1036
8. Vareda JP, Maximiano P, Cunha LP, Ferreira AF, Simões PN, Durães L (2018) Effect of different types of surfactants on the microstructure of methyltrimethoxysilane-derived silica aerogels: a combined experimental and computational approach. J Colloid Interface Sci 512:64–76
9. Zhang W, Tao Y, Li C (2018) Effects of PEG4000 template on sol-gel synthesis of porous cerium titanate photocatalyst. Solid State Sci 78:16–21
10. Thomson KT, Gubbins KE (2000) Modeling structural morphology of microporous carbons by reverse Monte Carlo. Langmuir 16:5761–5773
11. Family F, Landau DP (eds) (1984) Kinetics of aggregation and gelation. Elsevier, Amsterdam
12. Jullien R, Botet R (1987) Aggregation and fractal aggregates. World Scientific, Singapore
13. Jullien R, Hasmy A, Anglaret E (1997) Effect of cluster deformations in the DLCA modeling of the sol-gel process. J Sol Gel Sci Techn 8:819–824
14. Primera J, Woignier T, Hasmy A (2005) Pore structure simulation of gels with a binary monomer size distribution. J Sol Gel Sci Techn 34:273–280
15. Sorensen CM (2011) The mobility of fractal aggregates: a review. Aerosol Sci Technol 45:765–779
16. Meakin P, Djordjevic Z (1986) Cluster-cluster aggregation in two-monomer systems. J Phys A 19:2137–2153
17. Stoll S, Pefferkorn E (1996) Monte Carlo simulation of controlled colloid growth by homo- and heterocoagulation in two dimensions. J Colloid Interface Sci 177:192–197
18. Anderson ML, Morris CA, Stroud RM et al. (1999) Colloidal gold aerogels: preparation, properties, and characterization. Langmuir 15:674–681
19. AlSunaidi A, Lach-hab M, Gonzalez AE, Blaisten-Barojas E (2000) Cluster-cluster aggregation in binary mixtures. Phys Rev E 61:550–556
20. AlSunaidi A, Lach-hab M, Blaisten-Barojas E, Gonzalez AE (2000) Colloidal aggregation with mobile impurities. Phys Rev E 61:6781–6788
21. Woignier T, Primera J, Hasmy A (2006) Application of the diffusion limited cluster agregation model to natural gels: the allophanic soils. J Sol Gel Sci Techn 40(2-3):201–207
22. Meakin P (1983) Diffusion-controlled cluster formation in 2—6-dimensional space. Phys Rev Lett 51:1119–1122
23. Kolb M, Botet R, Jullien R (1983) Scaling of kinetically growing clusters. Phys Rev Lett 51:1123–1126
24. Hasmy A, Jullien R (1995) Sol-gel process simulation by cluster-cluster aggregation. J Non Cryst Solids 186:342–348